rection was the result of the purely odd light-polarization symmetry of the normal state in this direction for their samples. As we reported earlier (*20*), and confirmed in this study, our normal state for overdoped samples is of mixed symmetry. Our observation of a nonzero gap along the Γ-X direction for overdoped samples thus seems an intrinsic effect attributable to doping.

Several important conclusions stem directly from our data. Because the gap along the Γ-X direction is nonzero for the overdoped samples, such samples cannot possess a pure $d_{x^2-y^2}$ superconducting order-parameter symmetry. However, the optimally doped and underdoped samples exhibit a very small gap in the Γ-X direction, small enough to be consistent with pure $d_{x^2-y^2}$ symmetry.

We considered several possible models in light of our data. The extended *s*-wave model proposed by Varma and co-workers (*15*) indicates that the gap nodes would appear at different Brillouin zone locations as the size of the Fermi surface changes. We observed no change in the Fermi wave vector in the Γ-X direction between the two types of samples, indicating that this part of the Fermi surface did not appreciably change its size. Given that the change in Fermi surface might be smaller than our experimental uncertainty, however, we can neither rule out nor explicitly support an extended *s*-wave model.

Our present data are consistent with an anisotropic *s*-wave order parameter. However, the gap must become more anisotropic for underdoped samples; this experimental result will constrain such theoretical models. The data are also consistent with a two-component order parameter (*2*), with the relative weights of the two components changing with stoichiometry (*3*–*5*). Such models (*3*–*5*) predict that the gap minima (or nodes) change location as the relative weight of the two components changes. There is the possibility that the nodes in the gap function shift with doping (*13*, *14*). Because we measured the gap only along the high-symmetry directions, we can neither confirm nor exclude this possibility.

In summary, we have reproducibly and reversibly changed the superconducting gap anisotropy from ~20:1 to ~2:1 by changing the oxygen doping. The data distinguish among some theoretical models and constrain other models. Our data provide a solution for the apparent conflict between earlier photoemission reports as to whether there is a zero in the gap along the Γ-X direction in the Brillouin zone.

REFERENCES AND NOTES

1. R. J. Kelley *et al.*, *Phys. Rev. B* **50**, 590 (1994).
2. J. Ma *et al.*, *Science* **267**, 862 (1995).
3. J. Betouras and R. Joynt, *Europhys. Lett.* **31**, 119 (1995).
4. Q. P. Li *et al.*, *Phys. Rev. B* **48**, 437 (1993).
5. G. Kotliar, *ibid.* **37**, 3664 (1988).
6. S. D. Adrian *et al.*, *ibid.* **51**, 6800 (1995); A. G. Sun *et al.*, *Phys. Rev. Lett.* **72**, 2267 (1994); J. Buan *et al.*, *ibid.*, p. 2632.
7. D. A. Wollman *et al.*, *Phys. Rev. Lett.* **71**, 331 (1993).
8. W. N. Hardy *et al.*, *ibid.* **70**, 3999 (1993).
9. C. C. Tsuei *et al.*, *ibid.* **73**, 593 (1994).
10. Z.-X. Shen *et al.*, *ibid.* **70**, 1553 (1993).
11. The interpretation of (*10*) has been criticized by, for example, G. D. Mahan [*ibid.* **71**, 4277 (1993)].
12. R. J. Kelley *et al.*, *ibid.*, p. 4051.
13. H. Ding *et al.*, *ibid.* **74**, 2784 (1995).
14. H. Ding *et al.*, *ibid.* **75**, 1425 (1995).
15. C. M. Varma *et al.*, *ibid.* **63**, 1996 (1989); *ibid.* **64**, 497 (1990).
16. K. A. Müller, *Nature* **377**, 133 (1995).
17. P. D. Han and D. A. Payne, *J. Cryst. Growth* **104**, 201 (1990).
18. C. Kendziora *et al.*, *Physica C*, in press.
19. R. Fehrenbacher and M. R. Norman, *Phys. Rev. B* **50**, 3495 (1994); *Physica C* **235**, 2407 (1995).
20. J. Ma *et al.*, *Phys. Rev. B* **51**, 9271 (1995).
21. S. Massida *et al.*, *Phys. Lett. A* **122**, 197 (1987).

22. We benefited from conversations with I. Bozovic, J. Eckstein, R. Joynt, A. Chubukov, G. Varelogiannis, and V. Kresin. The staff at the Wisconsin Synchrotron Radiation Center (SRC), particularly R. Hansen and T. Baraniak, were most helpful. Financial support was provided by the U.S. National Science Foundation, both directly and through support of the SRC, École Polytechnique Fédérale Lausanne, Fonds National Suisse de la Recherche Scientifique, and the Deutsche Forschungsgemeinschaft.

28 July 1995; accepted 1 December 1995

Model Estimations Biased by Truncated Expansions: Possible Artifacts in Seismic Tomography

Jeannot Trampert* and Roel Snieder

In most linear imaging problems, where the model to be sought is expanded in a set of basis functions, it is common practice to truncate the set at a certain (arbitrary) level. The solution then depends on the chosen parameterization, and neglected basis functions may leak into the solution to produce artifacts in the retrieved model. An unbiased estimate of the coefficients of the true model may be obtained in the chosen finite basis set; here, a method to suppress leakage is illustrated on an example of global seismic tomography.

A linear inverse problem is defined as one in which the data are linear functionals of the model. Specifically, a datum, d_i, is related to the unknown model $m(\mathbf{r})$ by

$$d_i = \int G_i(\mathbf{r}) m(\mathbf{r}) d\mathbf{r} \qquad (1)$$

where $G_i(\mathbf{r})$ represents the known data kernels derived from theory. There are many ways of inferring models from data (*1*, *2*). We have restricted our discussion here to the convenient case where the model to be sought is expanded in a complete set of basis functions B_j such that

$$m(\mathbf{r}) = \sum_{j=1}^{\infty} c_j B_j(\mathbf{r}) \qquad (2)$$

Such an approach applies to a large class of interpolation, spectral analysis, and imaging problems in astronomy, geophysics, and medicine. Many different parameterizations (choices of basis functions) are possible, but as long as the chosen set is complete, they are all equivalent. To describe the model fully, the set of basis functions must be complete, and hence the summation in Eq. 2 has to be carried out to infinity. This would lead to an ill-posed inverse problem. In practice, we are limited by the finite resolution of the data, so that we have to choose an upper limit, L, for the expansion. This leads to a classical linear inverse problem for L coefficients, c_j, which may be represented by the matrix equation

$$\mathbf{d} = \mathbf{A}\mathbf{c} \qquad (3)$$

where the matrix $\mathbf{A}$ is defined by $A_{ij} = \int G_i(\mathbf{r}) B_j(\mathbf{r}) d\mathbf{r}$. The truncation of the expansion leads to a smoothed estimation of the true model, regardless of the real smoothness properties of the true model. Generally, we have no precise a priori knowledge of the unknown function $m(\mathbf{r})$, and our choice of L is guided by technical questions, such as the size of the inverse problem. Any real structure unrepresented by the finite number of basis functions fixed by L may produce a bias in our estimate of the low-order expansion of the true model.

We will show here that leakage may occur from neglected basis functions to the finite number of estimated coefficients and that inhomogeneous model sampling is responsible for this bias (*3*, *4*). We are thus confronted with the undesirable property that the model depends on the way it is sampled. We present here a mathematical formulation that takes the complete unknown model structure into account and suppresses leakage with the use of a weighted least-squares algorithm. The weighting ma-

J. Trampert, Ecole et Observatoire de Physique du Globe, URA 1358 ULP-CNRS, 5 Rue René Descartes, 67084 Strasbourg Cedex, France.
R. Snieder, Department of Theoretical Geophysics, University of Utrecht, P.O. Box 80.021, 3508 TA Utrecht, Netherlands.

*To whom correspondence should be addressed.

trix depends explicitly on the degree of truncation of the basis that has been chosen to parameterize the model. Using a global, surface-wave tomography problem, we will illustrate the effects of leakage and to what degree it can be suppressed.

A general least-squares solution (*1*) of Eq. 3 is obtained by minimizing the cost function

$$S_L = (\mathbf{d} - \mathbf{A}_L\mathbf{c}_L)^*\mathbf{C}_d^{-1}(\mathbf{d} - \mathbf{A}_L\mathbf{c}_L) + \mathbf{c}_L^*\mathbf{C}_{c,L}^{-1}\mathbf{c}_L \quad (4)$$

where the subscript L designates the truncation level of the set of basis functions and the superscript * denotes the matrix transpose. The operators $\mathbf{C}_d^{-1}$ and $\mathbf{C}_{c,L}^{-1}$ define norm weightings in data and model space, respectively, and the least-squares estimation of the first L model coefficients is given by

$$\mathbf{c}_L^{LS} = (\mathbf{A}_L^*\mathbf{C}_d^{-1}\mathbf{A}_L + \mathbf{C}_{c,L}^{-1})^{-1}\mathbf{A}_L^*\mathbf{C}_d^{-1}\mathbf{d} \quad (5)$$

Equation 3 can be decomposed into $\mathbf{d} = \mathbf{d}_L + \mathbf{d}_\infty = \mathbf{A}_L\mathbf{c}_L + \mathbf{A}_\infty\mathbf{c}_\infty$, where the subscript ∞ designates the neglected basis functions. This then in turn yields

$$\mathbf{c}_L^{LS} = (\mathbf{A}_L^*\mathbf{C}_d^{-1}\mathbf{A}_L + \mathbf{C}_{c,L}^{-1})^{-1}\mathbf{A}_L^*\mathbf{C}_d^{-1}\mathbf{A}_L\mathbf{c}_L + (\mathbf{A}_L^*\mathbf{C}_d^{-1}\mathbf{A}_L + \mathbf{C}_{c,L}^{-1})^{-1}\mathbf{A}_L^*\mathbf{C}_d^{-1}\mathbf{A}_\infty\mathbf{c}_\infty \quad (6)$$

The last term in Eq. 6 is responsible for the leakage, and it is readily shown that the basis functions are in general not orthogonal with respect to the product defined by $\mathbf{A}_L^*\mathbf{C}_d^{-1}\mathbf{A}_\infty$ (*3*). For a homogeneously sampled model, however, the inner product defining the orthogonality of the basis functions appears naturally, and the last term is close to zero (*4*). In the case of inhomogeneous sampling, $\mathbf{d}_\infty$ has a nonzero projection onto the space spanned by the first L basis functions, and leakage occurs. This leakage occurs because of an incomplete basis and inhomogeneous sampling, which are unfortunately common in inference problems. Leakage, however, can be suppressed if one is able to invert only that part of the data, $\mathbf{d}_L$, represented by L chosen basis functions.

This can in fact be done by minimizing the cost function

$$S_{tot} = (\mathbf{d} - \mathbf{A}_L\mathbf{c}_L - \mathbf{A}_\infty\mathbf{c}_\infty)^*\mathbf{C}_d^{-1}(\mathbf{d} - \mathbf{A}_L\mathbf{c}_L - \mathbf{A}_\infty\mathbf{c}_\infty) + \mathbf{c}_L^*\mathbf{C}_{c,L}^{-1}\mathbf{c}_L + \mathbf{c}_\infty{}^*\mathbf{C}_{c,\infty}^{-1}\mathbf{c}_\infty \quad (7)$$

which is obtained from Eq. 4 by replacing $\mathbf{c}_L$ with $\mathbf{c}_L + \mathbf{c}_\infty$, with the implicit condition that $\mathbf{c}_L$ and $\mathbf{c}_\infty$ are uncorrelated. Solving Eq. 7 gives rise to a system of two coupled linear equations in $\mathbf{c}_L$ and $\mathbf{c}_\infty$, which may be solved for $\mathbf{c}_L$ only, unbiased by the presence of $\mathbf{c}_\infty$. This procedure of partitioning the model or the data before inversion has been used in the past, and a general discussion of such techniques may be found elsewhere (*5*).

Minimizing S_{tot} gives a new estimation for $\mathbf{c}_L$:

$$\mathbf{c}_L^W = (\mathbf{A}_L^*\mathbf{W}\mathbf{A}_L + \mathbf{C}_{c,L}^{-1})^{-1}\mathbf{A}_L^*\mathbf{W}\mathbf{d} \quad (8)$$

with $\mathbf{W} = (\mathbf{A}_\infty\mathbf{C}_{c,\infty}\mathbf{A}_\infty^* + \mathbf{C}_d)^{-1}$. The anti-leakage operator, $\mathbf{W}$, appears as a weighting in the data space and undoes the effects of inhomogeneous sampling. Eqs. 5 and 8 have the same structure, and both results are maximum likelihood solutions given their respective norm weightings $\mathbf{C}_d^{-1}$ or $\mathbf{W}$. The difference in their solutions will be the fit to the data. Solutions to Eq. 8 will generally show a worse fit because only part of the data ($\mathbf{d}_L$) have been inverted, but these solutions will be unbiased by $\mathbf{d}_\infty$. Though the anti-leakage operator allows a priori errors and correlations to be incorporated into model and data space, the leakage reduction depends on these chosen norm weightings.

Most often one considers the case where $\mathbf{C}_d = \sigma_d^2\mathbf{I}$, $\mathbf{C}_{c,L} = \sigma_{c_L}^2\mathbf{I}$, and $\mathbf{C}_{c,\infty} = \sigma_{c\infty}^2\mathbf{I}$, with $\mathbf{I}$ being the identity matrix. These values in turn reduce Eq. 8 to

$$\mathbf{c}_L^W = [\mathbf{A}_L^*\mathbf{W}'\mathbf{A}_L + (\alpha^2/\beta^2)\mathbf{I}]^{-1}\mathbf{A}_L^*\mathbf{W}'\mathbf{d} \quad (9)$$

with $\mathbf{W}' = (\mathbf{A}_\infty\mathbf{A}_\infty^* + \beta^2\mathbf{I})^{-1}$, where $\alpha^2 = \sigma_d^2/\sigma_{cL}^2$ and $\beta^2 = \sigma_d^2/\sigma_{c\infty}^2$. The problem depends then on two constants; eigenvalue analysis gives insight into the importance of the chosen values for α^2 and β^2 to optimize leakage reduction (*6*). A crucial problem is the calculation of $\mathbf{A}_\infty\mathbf{A}_\infty^*$. Using the orthogonality between the different spaces involved, simple algebra leads to $\mathbf{A}_\infty\mathbf{A}_\infty^* = \Gamma - \mathbf{A}_L\mathbf{A}_L^*$, where $\Gamma_{ij} = \int G_i(\mathbf{r})G_j(\mathbf{r})d\mathbf{r}$ is the Gram matrix of the problem (*2*). The truncation level, L, appears explicitly in this expression. It is beyond the scope of this report to discuss the existence of Γ (not all inverse problems allow the evaluation of the Gram matrix) or the numerical problems involved in calculating an inverse matrix with the dimension of the data space. Another way of dealing with the leakage problem has been adopted by Backus (*7*) by holding hard prior bounds on the model. He showed that the finite number of basis functions, L, may be chosen so that all omitted basis functions, which satisfy the bound, cannot produce signals in the data that lie above the level of measurement error. In his terminology, we are suppressing leakage by using soft prior bounds.

Seismic tomography (*8–11*) is concerned with inferring the structure of the Earth (such as velocity or density) from data (such as arrival times or wave forms), and the frequently used linearized relation between the two is of the form of Eq. 1. The Earth model to be sought may be parameterized in many ways (such as spherical harmonics or cells) (*8–10*). Without any loss of generality, we will restrict the following discussion to a model parameterization in terms of spherical harmonics.

To illustrate the effects of leakage and of the anti-leakage operator, we simulated a seismic tomography experiment based on surface waves. We used a station-event distribution based on the global seismicity from 1989 together with the available global seismic stations (Fig. 1). We first computed synthetic data for a hypothetical Earth structure of spherical harmonic degree 10 and order 5 only (Fig. 2A). After adding 10% random noise, we inverted these data up to degree and order 8. Although the given ray coverage seems dense, significant spectral leakage (*12*) was present; the pure degree 10 structure leaves after inversion a significant imprint on the spherical harmonic coefficients up to degree and order 8 (Fig. 2B). The inversion based on Eq. 9 reduced the effects of leakage almost completely (Fig. 2C).

Next, we took the same ray geometry and computed synthetic data with 10% random noise for a hypothetical Earth structure of degree 5 and order 3 (Fig. 3A), which again we inverted up to degree and order 8. Results from Eqs. 5 and 9 were identical (Fig. 3, B and C), which indicates that the anti-leakage operator does not affect the lower degrees. This is different from a regularization approach. It would be possible to regularize the problem in such a way that leakage is suppressed, but that would also affect the lower degrees. There would then be a trade-off between leakage reduction and resolution. The anti-leakage operator keeps per-

Fig. 1. Rayleigh wave coverage for 1989 used in this study. Blue rays indicate minor arc paths and orange lines indicate major arc paths.

fect resolution for the lower degrees.

Many three-dimensional seismic models have been developed so far. A recent comparison of global tomographic models (*11*) shows that although the degree of correlation is encouraging, many discrepancies remain. None of the global tomographic models has the ability to resolve small structures (that is, these models are predominantly long wavelength models); only recently have some researchers suggested that important, small-scale structure might have been omitted in these long wavelength models (*13*) or, worse, that such omissions might be responsible for a certain amount of bias (*3*). With the accumulation of digital seismograms in worldwide data centers and the possibility to treat all available information automatically (*14*), it seems clear that the power spectrum of Earth's structure is whiter than has previously been assumed.

With the above theory, it has become possible to analyze the effects of leakage on existing global three-dimensional seismic models. We took a Rayleigh wave phase velocity model (*14*) for a period of 80 s expressed in terms of spherical harmonics up to degree and order 20 and computed synthetic data for the ray geometry depicted in Fig. 1. We added 10% random noise to the data and inverted it with a classical least-squares algorithm (Eq. 5), assuming the real Earth has only an aspherical structure up to degree and order 12 and thus neglecting a considerable amount of power. The inferred model (Fig. 4B) deviates from the true model (Fig. 4A) in amplitude and geographical position. The main differences occurred in the signature of the mid-Atlantic ridge and in a pronounced low-velocity feature in southern Africa that is clearly not present in the initial model. The magnitude of these differences was of the same order as the discrepancies described in (*11*). The model inferred with the anti-leakage operator of Eq. 9 (Fig. 4C) is almost indistinguishable from the true model.

These results suggest that the small-scale structure omitted in existing three-dimensional Earth models may be responsible for some differences on current tomographic models. The bias toward long wavelengths that occurs in these models by neglecting small-scale structure is reminiscent of "aliasing" (*15*). But leakage and aliasing are quite different. Aliasing occurs when the structure is undersampled (evenly or unevenly) by the data. Once the undersampling has occurred, nothing can be done to correct for aliasing. Leakage occurs because the basis functions are not orthogonal with respect to the matrix products involved in

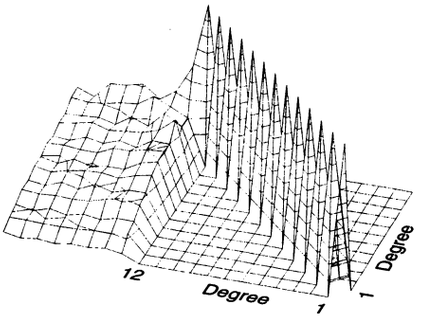

Fig. 5. The estimated model (degrees 0 through 12) is a filtered version of the true model (degrees 0 through 20). The square defined by degrees 0 through 12 by 0 through 12 is the classical resolution matrix, which is close to unity because of the a priori information. The rectangle defined by degrees 0 through 12 by 13 through 20 describes the bias. The lower the degree, the less it is biased by the neglected basis functions; the higher the neglected degree, the less it leaks.

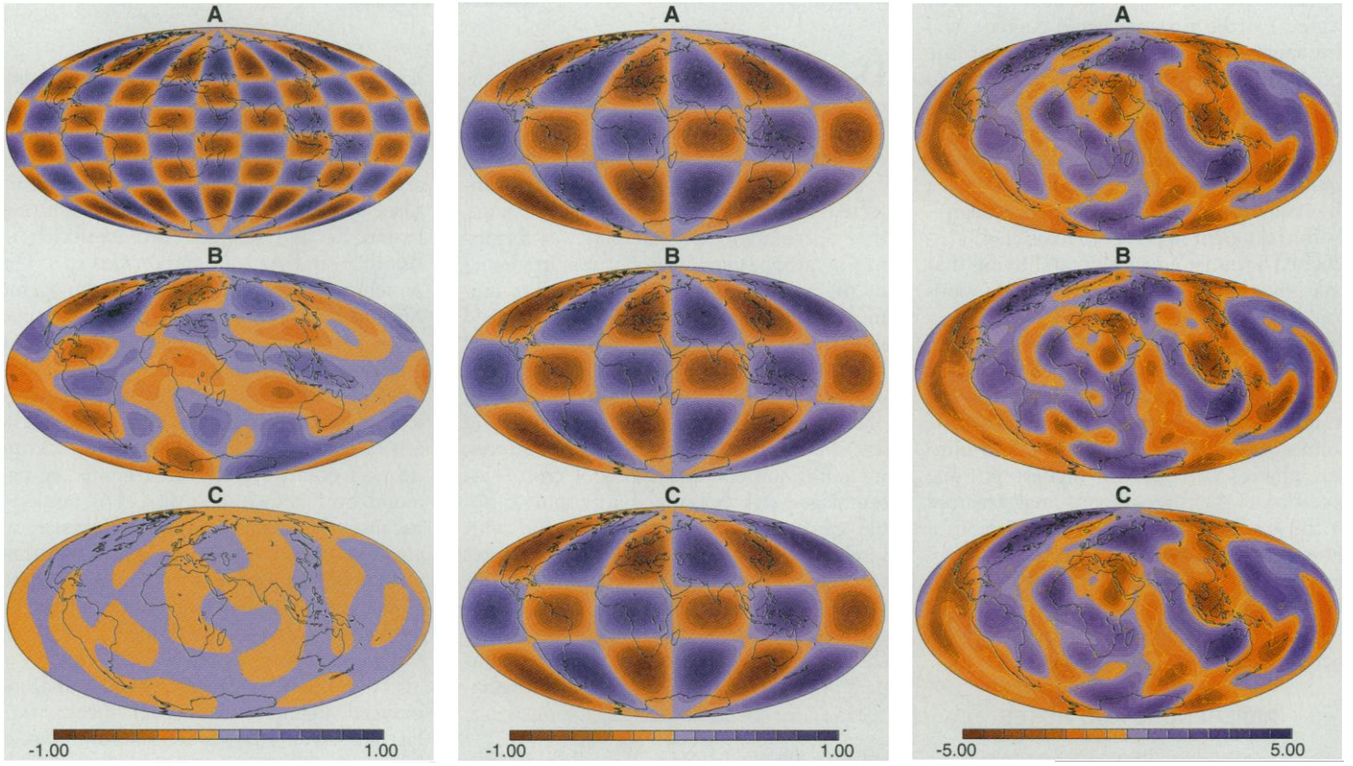

Fig. 2 (left). Synthetic experiment: Inversion of a pure degree 10 structure (**A**) with a classical least-squares algorithm (**B**) and anti-leakage algorithm (**C**) up to degree and order 8. The scale is relative to unit input. **Fig. 3 (center).** Synthetic experiment: Inversion of a pure degree 5 structure (**A**) with a classical least-squares algorithm (**B**) and anti-leakage algorithm (**C**) up to degree and order 8. The scale is relative to unit input. **Fig. 4 (right).** Realistic experiment: A Rayleigh wave phase velocity model (*14*) at a period of 80 s was used to calculate synthetic data up to degree and order 20. (**A**) The true degree 12 reference model. The data were then inverted with a classical least-squares algorithm (**B**) and anti-leakage algorithm (**C**) up to degree and order 12. All phase velocity perturbations are in percent and relative to PREM (*18*). The main differences occur at the mid-Atlantic ridge and in southern Africa. The neglected power of degrees 13 through 20 present in the data is responsible for the bias.

the inverse problem, in the case of uneven sampling only. Aliasing takes place only from small-scale signals to long wavelength signals, whereas leakage may occur both ways. For instance, in the determination of magnetic anomaly maps, it is common to expand the anomaly field into spherical harmonic degrees 15 through 60 (*16*). Without any precautions, there is a possibility of leakage from low-frequency basis functions (below degree 15) as well as from high-frequency basis functions (above degree 60).

Another, more general, way of looking at the effects of leakage is by considering Eq. 6. The first term of the right-hand side defines the classical resolution operator. The additional term on the right-hand side defines the bias introduced by leakage, and its interpretation is similar to that of the resolution operator. It is clear from its expression that the bias operator depends on only the sampling geometry by means of the data kernels and the a priori information (or norm weightings). We calculated the bias operator for the tomography problem discussed above for spherical harmonic degrees 13 through 20. Figure 5 shows the bias operator together with the resolution operator for each degree. Degree 12 (the highest degree of the expansion) is most biased by degree 13 (the first neglected degree), and the spectral leakage is strongest for the spherical harmonic components close to the truncation level. Whereas the weighted least-squares model is almost identical to the true model, the classical least-squares model departs more and more from the true model with each higher degree. With a different approach, Hulot *et al.* (*17*) reached a similar conclusion and found that only the lowest degrees of core motions could be retrieved satisfactorily from geomagnetic data.

The far-reaching conclusions of seismic tomography in terms of geodynamic constraints on the driving forces of mantle convection, petrological models, and mineral physics call for the highest possible precision of the three-dimensional structure of the Earth's interior. The formulation of most seismic tomography problems introduces a bias by leaking basis functions into the solution (Figs. 4 and 5). Accounting for such leakage might change our three-dimensional image of the Earth.

REFERENCES AND NOTES

1. A. Tarantola, *Inverse Problem Theory: Methods for Data Fitting and Model Parameter Estimation* (Elsevier, New York, 1987).
2. R. L. Parker, *Geophysical Inverse Theory* (Princeton Univ. Press, Princeton, NJ, 1994).
3. R. Snieder, J. Beckers, F. Neele, *J. Geophys. Res.* **96**, 501 (1991).
4. R. Snieder, in *Seismic Tomography: Theory and Practice*, H. M. Iyer and K. Hirahara, Eds. (Chapman and Hall, London, 1993), pp. 23–63.
5. C. Spencer, *Geophys. J. R. Astron. Soc.* **80**, 619 (1985).
6. For leakage reduction to be optimal, values for α^2 have to be smaller than those for β^2 without reaching 0. In all our simulations, we used $\alpha^2 = 10^{-6}$ and $\beta^2 = 10^{-3}$.
7. G. E. Backus, *Geophys. J.* **92**, 125 (1988).
8. A. M. Dziewonski and J. H. Woodhouse, *Science* **236**, 37 (1987).
9. J. H. Woodhouse and A. M Dziewonski, *Philos. Trans. R. Soc. London Ser. A* **328**, 291 (1989).
10. B. A. Romanowicz, *Annu. Rev. Earth Planet. Sci.* **19**, 77 (1991).
11. M. H. Ritzwoller and E. M. Lavely, *Rev. Geophys.* **33**, 1 (1995).
12. D. Giardini, X.-D. Li, and J. H. Woodhouse [*J. Geophys. Res.* **93**, 13716 (1988)] worried about the truncation of basis functions in seismic tomography by using normal modes. Snieder *et al.* (*3*) analyzed the origin of the leakage. They referred to the problem as "spectral leakage" because their whole analysis used a spectral basis (spherical harmonics).
13. O. Gudmundsson, J. H. Davis, R. W. Clayton, *Geophys. J. Int.* **102**, 25 (1990).
14. J. Trampert and J. H. Woodhouse, *ibid.* **122**, 675 (1995).
15. R. Bracewell, *The Fourier Transform and Its Applications* (McGraw-Hill, New York, 1965).
16. J. Arkani-Hamed, R. A. Langel, M. Purucker, *J. Geophys. Res.* **99**, 24075 (1994).
17. G. Hulot, J. L. Le Mouël, J. Wahr, *Geophys. J. Int.* **108**, 224 (1992).
18. A. M. Dziewonski and D. L. Anderson, *Phys. Earth Planet. Inter.* **25**, 297 (1981).

19. We would like to thank A. Jackson and J. Woodhouse for many stimulating discussions at earlier stages of this work. J.-J. Lévêque provided many useful comments during the preparation of this manuscript.

17 October 1995; accepted 16 January 1996

Radiation-Induced Diamond Formation in Uranium-Rich Carbonaceous Materials

Tyrone L. Daulton* and Minoru Ozima

Nanometer-sized diamonds were identified by transmission electron microscopy in a uranium-rich, coal-like carbonaceous assemblage of Precambrian age. This observation, together with estimates of formation efficiencies, supports the hypothesis that diamond can form in carbonaceous material irradiated by the radioactive decay products of uranium. The results also suggest that the formation of carbonados cannot be sufficiently explained by a radiation mechanism alone.

Dubinchuk *et al.* (*1*) first reported submicrometer-sized diamonds in uranium-bearing sedimentary rocks with a high carbon content (for example, kerogens, lignite, coal, and kerite) that had never been subjected to high temperatures or pressures; they speculated that diamond was formed when carbonaceous material was irradiated by the spontaneous fission products of uranium. Kaminsky (*2*) extended this idea and proposed that carbonados were also formed by this mechanism. Carbonados are polycrystalline porous aggregates of fine-grained diamonds found only in placer deposits and are characterized by many crustal features, including mineral inclusions of crustal assemblages, tightly trapped atmospheric noble gases, and a lack of association with kimberlites or lamproites. These features strongly suggest that the diamonds did not form by high static pressure in Earth's mantle. One possible mechanism of formation is shock metamorphism resulting from the impact of extraterrestrial bodies (*3*). Carbonados containing the shock-associated diamond polymorph lonsdaleite have been found in meteorite craters (*4*). However, not all carbonados contain lonsdaleite or are associated with established impact structures. A considerable amount of parentless fission Xe and Kr has been identified in Brazilian and African carbonados (*5*). The presence of such large amounts of fissiogenic Xe and Kr is possible only if the carbonaceous precursors to diamond (as well as the diamond itself) were originally part of a finely dispersed U-rich material over geological time scales, consistent with the hypothesis of Kaminsky (*2*). However, the identification of micrometer-sized grains as diamond by Dubinchuk *et al.* (*1*) is tenuous, because the determination was based on electron microdiffraction patterns that yielded unit-cell parameters similar to those of diamond. No stereographic analysis of the diffraction patterns or chemical analysis of the grains was reported.

To evaluate the feasibility of a radiation-induced diamond formation mechanism, Fisenko *et al.* (*6*) studied carburanium, a U-rich (~5% uranium oxides by weight), fine-grained, coal-like assemblage containing hydrous, amorphous carbonaceous material (~65% by weight) of Precambrian age (1.7 ± 0.2 billion years) from North Karelia, Russia (*7*). The carbonaceous grains in carburanium have received high

T. L. Daulton, Department of Physics and McDonnell Center for the Space Sciences, Washington University, St. Louis, MO 63130, USA.
M. Ozima, Department of Earth and Planetary Sciences, Washington University, St. Louis, MO 63130, USA, and Department of Earth and Planetary Physics, University of Tokyo, Bunkyo-Ku, Tokyo 113, Japan.

*To whom correspondence should be addressed. Present address: Materials Science Division, Argonne National Laboratory, Argonne, IL 60439, USA.